Chinese Journal of Polymer Science Vol. 33, No. 11, (2015), 1625–1632

Chinese Journal of Polymer Science
© Chinese Chemical Society
Institute of Chemistry, CAS
Springer-Verlag Berlin Heidelberg 2015

The Banded Spherulites of *i*PP Induced by Pressure Vibration Injection Molding

Ren-xi La, Qi-xiong Zhou, Chao Xia, Da-shan Mi and Jie Zhang*
State Key Laboratory of Polymer Materials Engineering, College of Polymer Science and Engineering, Sichuan University, Chengdu 610065, China

Abstract Isotactic polypropylene (*i*PP) samples obtained by pressure vibration injection molding (PVIM) and conventional injection molding (CIM) were studied by polarized-light microscopy (PLM), respectively. It was found that the alternating bright and dark banded spherulites were generated in the transitional region of PVIM parts. It is the first time that the banded spherulites of isotactic polypropylene were observed in polymer processing. What's more, the banded spherulites were proved to be constituted of α-form crystal by hot stage polarized-light microscopy (HT-PLM) and wide angle X-ray diffraction (WAXD). Morphology of the banded spherulites was also studied by scaning electronical microscopy (SEM).

Keywords: α-Form *i*PP; Banded spherulites; Vibration injection molding; Oscillatory pressure.

INTRODUCTION

Banding is a common feature for the crystallizable polymer, especially for polyethylene[1–11] and polyesters[12, 13] in melt or dilute solution crystallization. It is usually testified by a concentric rings pattern from testing methods of polarized light microscopy (PLM), scanning electron microscopy (SEM) and atomic force microscopy (AFM). According to the formation mechanism suggested in the literatures[14–22], there are two main theories to explain the banding phenomenon. One tends to elucidate the phenomenon by the stepwise crystallization (or rhythmic crystallization) in which changing crystallization conditions lead to different crystalline morphology even in a single spherulite, the other, however, attributes the formation of banding to collaborative twisting of lamellae along the radial direction during the growing process of spherulites. As to the lamellar twisting mechanism of spherulites, it was referred to two models. One model was originally proposed by Schultz and Kinloch[14] and then modified by Bassett[15–17] and his co-worker in great detail. They insisted that the overall twist of the radial growing lamellae was initiated by transverse screw dislocations with the same sign so that the banding extinction pattern was observed under PLM. The diverse translation of the molecules that stems from screw dislocations was attributed to cilia irregularity associated with the fold surfaces of neighboring lamellae. The other was initially proposed by Keller[18] and developed intensively by Keith and Padden[2, 19, 20]. They suggested that the twisting of lamellar was attributed mainly to the influence of the unbalanced surface stress resulting from the asymmetry of lamellar geometry. Singfield[21] considered that although the two theories regarding lamellae twisting were different from each other, they still had much in common since they all pointed out the need for some kind of asymmetry to create a periodically oriented variation or "twist" of the growing lamella.

Isotactic polypropylene, which has complex and multifaceted crystalline architecture, is capable of

* Corresponding author: Jie Zhang (张杰), E-mail: zhangjie@scu.edu.cn
Received May 8, 2015; Revised June 26, 2015; Accepted July 1, 2015
doi: 10.1007/s10118-015-1708-x

crystallizing in different unit cell modifications, including α-, β-, γ-crystal phases. Padden and Keith[3] used thin films to crystallize in a temperature range from 110 °C to 148 °C and observed a variety of spherulite appearances which were classified as five distinct types. It is known that formation of unique cross-hatched lamellae of α-*i*PP spherulites is the result of homoepitaxial growth of lamellar branches, and then the tangential lamellae grow epitaxially on radial lamellae[23–25]. The transformation in birefringence of three types of α- spherulites is attributed to the relative amount of tangential lamellae in the crosshatched structures.

It is generally believed that in the α- form spherulite lamellae grow in a planar way, therefore banding phenomenon induced by lamellar twisting can not be realized. Nevertheless, Lotz and Cheng[22] have made a elaborated summary about recent works of research teams and considered that unbalanced surface stresses resulted from differential congestion of folded surfaces is the vital factor for the mechanical origin of twisting and scrolling of lamellae. Yiguo Li[26] has found the dominate role of structural feature on lamellar twisting and the significant influence of crystallization condition on lamellar packing along the radial direction of spherulites by controlling solvent evaporation in solution-cast film.

While banded spherulites form normally through crystallization in melt or dilute solutions, they are rarely obtained during polymer processing. Through considerable efforts, some researchers have gained banded spherulites of PE in extrusion[27] and gas-assisted injection molding[28]. However, banded spherulites of *i*PP have never been reported in the processing condition yet to the best of our knowledge. In this paper, we prepared *i*PP samples by a home-made pressure vibration injection molding (PVIM) device[29], on the contrast to the conventional injection molding device, beside the packing pressure, it has an advantage of adding additional oscillatory pressure transmitted into the mold cavity during the packing stage. To see the characteristics of banded spherulites of *i*PP, we performed PLM measurements on the samples after they were prepared. In addition, hot stage polarizing light microscopy (HT-PLM), wide angle X-ray diffraction (WAXD) and scaning electronical microscopy (SEM) were done to check the morphology of banded spherulies in *i*PP.

EXPERIMENTAL

Materials

The isotactic polypropylene homopolymer employed in this work was a commercial product of Lanzhou Petroleum Chemical Co. (China). The number-average molecular weight (M_n) determined by gel permeation chromatography (GPC) was 1.1×10^5 g/mol and its melt flow index (MFI) was 2.5 g/10 min.

Samples Preparation

*i*PP was injected into the mold using PVIM. During the process, the injection ram was driven by a vibration and an injection systems. The injection system provides a basic pressure while the vibration system provides an oscillatory pressure. During the packing stage, the periodically changing pressure acts on the melt in the runner and mold cavity until the injection gate is frozen. A schematic representation of the melt vibration injection apparatus is shown in Fig. 1 and the processing parameters are shown in Table 1. For the purpose of comparison, conventional injection molding (CIM) was carried out under static packing (without vibration) by using the same processing parameters. The samples were dumbbell-shaped, as shown in Fig. 2.

Table 1. The relevant parameters for processing

	Vibration pressure (MPa)	Vibration frequency (Hz)	Melting temperature (°C)	Injection and packing pressure (MPa)	Mould temperature (°C)
PVIM	55	1.43	230	35	60
CIM	–	–	230	35	60

Morphology of the vibration and static specimens was observed with the aid of polarized-light microscopy (PLM). The specific preparing process of microtomed slice was schematized in Fig. 2. Subsequently, micrographs of the slice were taken using a DX-1 (Jiang Xi Phoenix Optical Co. China.) microscope connecting

to a Nikon 500D digital camera. Hot stage was employed to investigate the melting behavior of the same slice. The slice was heated from the room temperature to 180 °C at a rate of 10 K/min and held for 2 min, then cooled to room temperature again at a rate of 20 K/min.

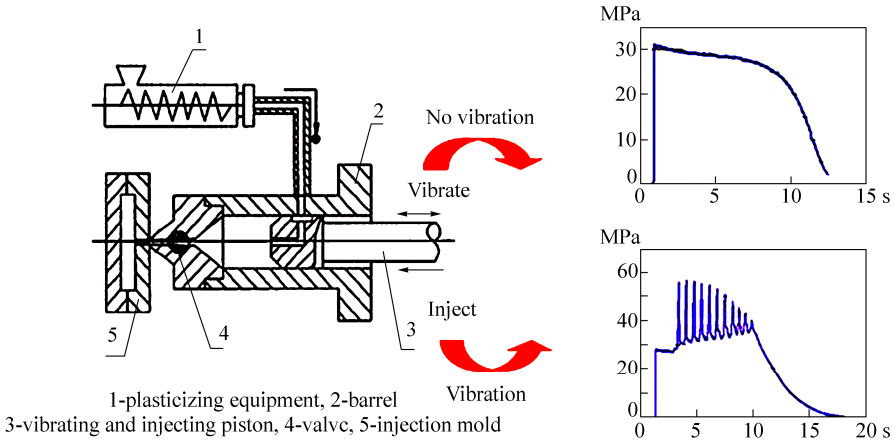


Fig. 1 Schematic representation of pressure vibration injection molding and the pressure change in the mold cavity

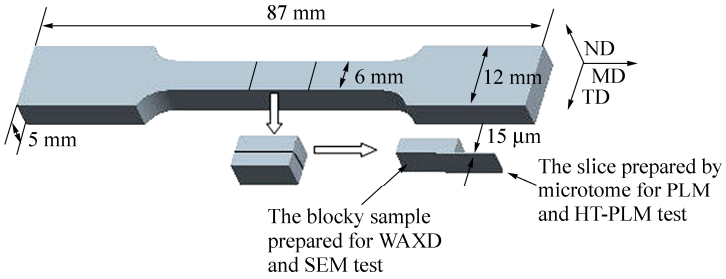


Fig. 2 Sketch of part obtained by PVIM, CIM and the schematic of position of the sample for test (MD, the flow direction; TD, the transverse direction; ND, the direction normal to the MD-TD plane)

The WAXD measurements were carried out at room temperature with a Rigaku D/diffractometer with curved graphite crystal filtered Cu Kα radiation source (λ = 0.154 nm) at 35 kV and 20 mA. The range of diffraction angle was from 5° to 35° and the scanning rate was 0.03 (°)/min.

For the SEM observation, the PVIM sample was ground and polished to reach the same thickness as the sliced ones prepared for polarized light microscopy, then we etched sample for a certain time in an etchant consisting of a 3% *W/V* potassium permanganate solution with sulphuric and orthophosphoric acids in it, and then washed with 30% hydrogen peroxide and distilled water. The sample was gold sputtered before the observation.

RESULTS AND DISCUSSION

Figure 3 shows micrographs of CIM and PVIM samples under polarized light microscope. According to Viana[30] CIM sample can be divided into three regions. From the surface to the center they are skin region, transition region and core region respectively as shown in Fig. 3(a). The skin region starts forming during the filling stage due to the rapid cooling when oriented melt contacts with the cold mold surface. The core region lies in the center of the sample. It is composed of typical spherulites because in this region crystallization takes place under quiescent and slow cooling condition. Transition region that lies between the skin region and the core region forms in the packing stage. In this region, deformed spherulites are frequently observed because relatively weaker shear effect on melt before or/and during crystallization. Different from the CIM sample,

another layer-like structure (shown on Fig. 3c) which is parallel to the flow direction is located at the outer portion of the transitional region in the PVIM sample. Considering the location of the specific layer-like structure and the feature of PVIM, we believe that it was induced by oscillatory shear effect during the early packing period.

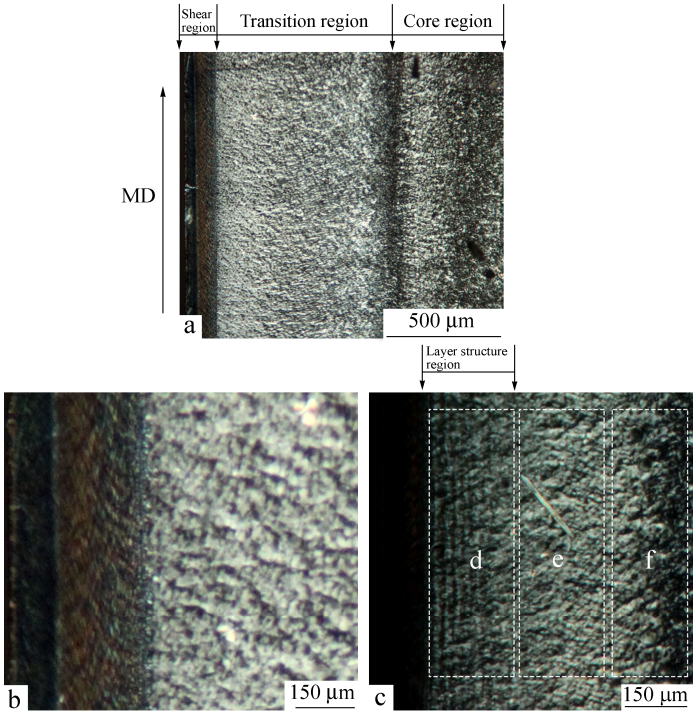


Fig. 3 PLM micrographs of samples with low magnification: (a) CIM sample observed with magnification of 40x, (b) CIM sample observed with magnification of 100x and (c) PVIM sample observed with magnification of 100x (The regions d, e, f marked by dot lines are specially investigated with high magnification in Fig. 4.)

To obtain more detailed information within the transition region of samples, different region of the PVIM sample are investigated under higher magnification (400x), as shown in Fig. 4. As discussed before, deformed spherulites mainly observed in the transition region of CIM samples. Surprisingly, comparing with CIM samples, large amount of banded spherulites are acquired in almost the whole transition region of PVIM samples. Figures 4(d), 4(e) and 4(f) are captured at higher magnification from the outer, middle and inner portions of the transitional region which are named as d, e and f region(marked by dotted box) in Fig. 3(c) respectively. The alternating dark and bright concentric bands of the banded spherulites can be clearly classified in these pictures. Moreover, It is a progressive development for the banded spherulites from outside portion to inside portion. In the inner portion (Fig. 4f) the size of banded spherulites are large, the distance between each band is narrow and having high band density in each spherulite. However, the phenomenon found in the outer portion is completely opposite. More interesting is the bands of the smaller banded spherulites appearing inside and near the layer-like structure present a polygonal (rather than round shape) appearance, as shown in Fig. 4(d). Even in the center of layer-like structure, the band shape of larger banded spherulites is polygonal as well.

At first, we speculated these banded spherulites to be the β_{IV} type, in respect that β spherulite is polygonal in its early crystallization stage according to Varga' observation and β_{IV} type is the only banded type among the five types of *i*PP spherulites. In order to confirm what modification these banded spherulites belong to, WAXD was applied on the microtomed sample for twice, as shown in Fig. 5. According to the theory of Natta[31] *et al.* and Turner-Jones[32] *et al.*, in the WAXD picture the marked peaks for α-modification crystal are located at 2θ = 14°, 17°, 18.5°, 21° and 22° respectively, while those for the β-modification crystal are located at 2θ = 16° and

21° respectively. As shown in Fig. 5, the intensity of the β- modification crystal at $2\theta = 16°$ is rather weak. If the banded spherulites is β-modification, the intensity of β crystal diffraction peak should be much stronger, because almost the whole transition region is covered with banded spherulites. So it is clear that these banded spherulites belong to α-modification.

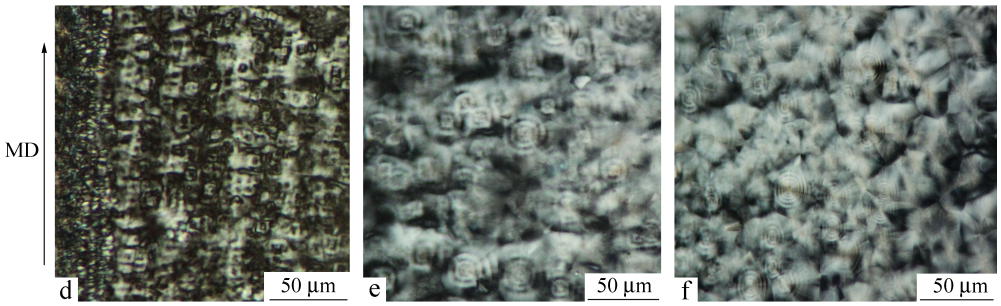


Fig. 4 PLM micrographs of PVIM samples obtained in the different transition regions with high magnification: (d) outer portion, (e) middle portion and (f) inner portion

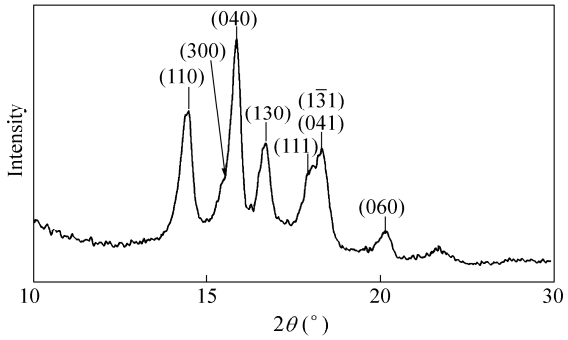


Fig. 5 1D WAXD powder pattern of PVIM sample

To determine the melting behaviors of the banded spherulites, the sample was heated on the hot stage connecting to the polarized light microscope (HTPLM). The photos were taken at intervals and shown in Fig. 6. The β-modification spherulite marked by the black circle is surrounded by serveral banded spherulites and is of high brightness. The β-modification spherulite begins to melt at 140 °C and disappears at about 145 °C, while the alternating dark and bright bands remain survived in sight. With increment of temperature, the banded spherulites begin to melt at 160 °C, and disappear at about 165 °C. This result indicates that banded spherulites have better heat stability than β-modification spherulite and they have the same melting behavior as ordinary α-modification spherulites. So it is once again testified that the banded spherulite is belong to α type. When the sample is cooled down to room temperature under quiescent condition, only the ordinary α-modification spherulites are in sight, as shown in Fig. 6(d).

In order to further investigate the morphology of the banded spherulites, etching technique and field emission SEM are employed. Comparing with the morphology of normal α-modification spherulite, the banded spherulites under SEM which marked by black dot line in Fig. 7(a) have the similar appearance with the ones observed under optical microscope. Moreover, as shown in Fig. 7(b) it has so called bright ‘peaks’ and dark ‘valleys’ structure, which is quite similar to the commonly mentioned banded spherulite formed by collaborative twisting of the lamellae, indicated that there are branches or twisting within the lamellae.

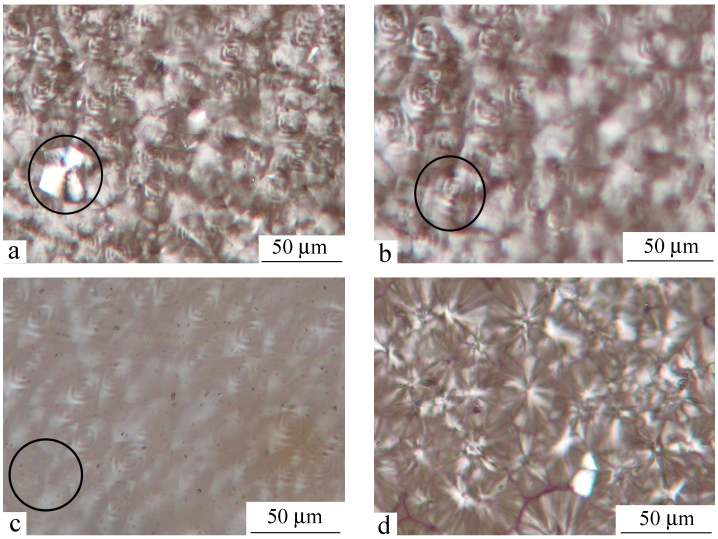


Fig. 6 Melting behavior of the banded spherulites and β-form crystal: (a) sample observed at room temperature, (b) sample heated at the temperature of 146 °C, (c) sample heated at the temperature of 160 °C and (d) sample cooled to room temperature after heating

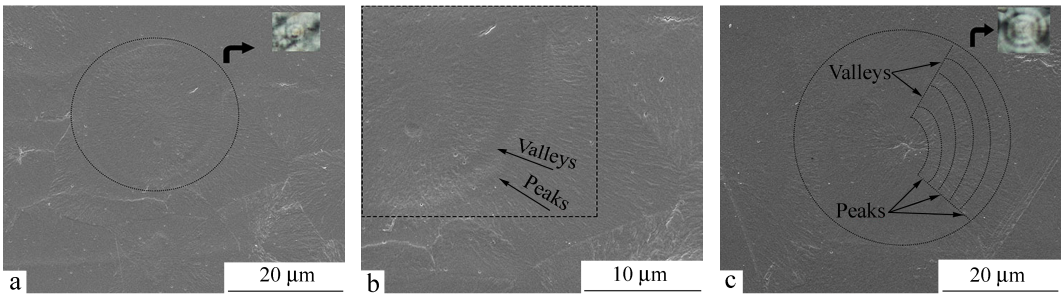


Fig. 7 SEM images of two different banded spherulites after etching: (a) the banded spherulites with a single "band", (b) unique 'peaks' and 'valleys' structure at lower right corner of the banded spherulite from Fig. 7(a) observed at high magnification and (c) the banded spherulites with two "bands" (The pictures imbedded in upper right of the photos show PLM images of the correpongding banded spherulites.)

Due to the following facts, the density of tangential lamella grown epitaxially on radial lamella is influenced by the crystallization condition, and oscillatory pressure exerts on the melt during the packing stage of PVIM, so we postulate that the formation mechanism of the banded spherulite found in our experiment belongs to the stepwise crystallization. It is expected to be explained by competition of growth of different oriented lamellae within cross-hatched structure after imposing of periodical pressure. Periodical pressure induced a periodical stress field in the melt, by which growth of lamellae was affected. When the vibration stress is high, the tangential lamellae is more apt to grow epitaxially on radial lamellae, causing density of tangential lamellae is relatively higher. While pressure is low, in other words, as relaxation of vibration pressure, the radial lamellae is preferentially developed. With periodically change of density for both radical and tangential lamellae, the birefringence in a single spherulite is also transformed, going from probably negative to zero, then negative, then zero, *etc*. Otherwise, the reason for hierarchical transformation of morphology of the banded spherulites (shown in Figs. 4d, 4e, 4f respectively) can be attributed to attenuation of vibration pressure. Within the inner portions of transitional region (Fig. 4f), the transmission of vibration reaches its highest value so that it is capable of maintaining longer time to induce more "bands" structure. Whereas, with the decrement of distance to the surface of sample (shown in Figs. 4d, 4e), effect of vibration pressure is gradually weakened and making less time for applying the vibration pressure. Hence, less "bands" are formed in the banded spherulies. However, the

above discussion can not interpret all the phenomenon of banded spherulites we observed, further investigation is now being carried on.

CONCLUSIONS

The morphologies of *i*PP samples prepared by the conventional injection molding (CIM) and pressure vibration injection molding (PVIM) were investigated using PLM, WAXD and SEM. Several conclusions could be drawn from the experimental results.

1. All samples can be divided into three regions: skin region, transition region and core region. There is no obvious difference in the skin region and core region comparing the micrographs of CIM and PVIM samples under polarized light microscopy. However, in the PVIM sample a layer-like structure which is parallel to the flow direction is observed in the outer portion of transitional region, which is mainly induced by oscillatory shear effect in the early packing period.

2. It is the first time that banded spherulites were observed in the processing. In the inner portion of transitional region the size of banded spherulites are much larger, the band space is narrower, while in the outer portion the condition is quite opposite. The banded spherulites have better heat stability than the β-modification spherulites after heating. The alternating dark and bright banded spherulites melt almost at the same time (about 160 °C), and have the same melting behavior as the ordinary α-modification spherulite. Moreover, the banded spherulite image taken by SEM has the similar appearance to the ones observed by optical microscope, which has a structure with bright ‘peaks’ and dark ‘valleys’.

3. We postulated a formation mechanism of the banded spherulites in our experiment. It could be induced by periodically changes in the density of tangential lamella under the oscillatory pressure. And the birefringence of spherulites also varies with it, so that optical alternating banded spherulites can be observed by PLM.

REFERENCES

1 Point, J., J. Bull. Classe. Sci. Acad. Roy. Belg., 1955, 41: 982
2 Keith, H.D. and Padden, F.J., J. Polym. Sci., 1959, 39(135): 123
3 Keith, H.D., Padden, F.J., Walter, N and Wyckoff, H.J., J. Appl. Phys., 1959, 30(10): 1485
4 Keller, A.J., J. Polym. Sci., 1959, 39(135): 151
5 Price, F.P., J. Polym. Sci., 1959, 39(135): 139
6 Keller, A. and Sawada, S., J. Makromol. Chem., 1964, 74(1): 190
7 Palmer, R. and Cobbold, A., J. Makromol. Chem., 1964, 74(1): 174
8 Barham, P. and Keller, A.J., J. Mater. Sci., 1977, 12(11): 2141
9 Saracovan, I., Keith, H.D., Manley, R.S.J. and Brown, G., Macromolecules, 1999, 32(26): 8918
10 Janimak, J., Markey, L. and Stevens, G., Polymer, 2001, 42(10): 4675
11 Lustiger, A., Lotz, B. and Duff, T.J., J. Polym. Sci., Part B: Polym. Phys., 1989, 27(3): 561
12 Kawashima, K., Kawano, R., Miyagi, T., Umemoto, S. and Okui, N.J., J. Macromol. Sci. Phys., 2003, 42(3–4): 889
13 Keith, H.D. and Padden, F.J., Macromolecules, 1996, 29(24): 7776
14 Schultz, J. and Kinloch, D., Polymer, 1969, 10: 271
15 Bassett, D. and Hodge, A., Polymer, 1978, 19(4): 469
16 Bassett, D. and Vaughan, A., Polymer, 1985, 26(5): 717
17 Bassett, D., Olley, R. and AlRaheil, I., Polymer, 1988, 29(9): 1539
18 Keller, A.J., J. Polym. Sci., 1955, 17(84): 291
19 Keith, H.D. and Padden, F.J., J. Polym. Sci., 1959, 39(135): 101
20 Keith, H.D. and Padden, F.J., Polymer, 1984, 25(1): 28
21 Singfield, K., Hobbs, J. and Keller, A.J., J. Cryst. Growth, 1998, 183(4): 683

22 Lotz, B. and Cheng, S.Z.D., Polymer, 2005, 46(3): 577
23 Padden, F.J. and Keith, H.D., J. Appl. Phys., 1966, 37(11): 4013
24 Binsbergen, F. and DeLange, B., Polymer, 1968, 9: 23
25 Lovinger, A.J.J., J. Polym. Sci., Part B: Polym. Phys., 1983, 21(1): 97
26 Li, Y., Huang, H., Wang, Z. and He, T., Macromolecules, 2014, 47(5): 1783
27 Trifonova, D., Drouillon, P., Ghanem, A. and Vancso, G.J., J. Appl. Polym. Sci., 1997, 66(3): 515
28 Huang, L., Yang, W., Yang, B., Yang, M., Zheng, G. and An, H., Polymer, 2008, 49(19): 4051
29 Zhang, J., Shen, K., Na, S. and Fu, Q., J. Polym. Sci., Part B: Polym. Phys., 2004, 42(12): 2385
30 Viana, J.C., Cunha, A.M. and Billon, N., Polymer, 2002, 43(15): 4185
31 Natta, G. and Corradini, P., J. Il Nuovo Cimento (1955–1965), 1960, 15: 40
32 Jones, A.T., Aizlewood, J.M. and Beckett, D., J. Makromol. Chem., 1964, 75(1): 134